

SCIENTIFIC REPORTS



OPEN

Nonfunctional ingestion of plant miRNAs in silkworm revealed by digital droplet PCR and transcriptome analysis

Received: 03 February 2015

Accepted: 19 June 2015

Published: 21 July 2015

Ling Jia, Dayan Zhang, Zhonghuai Xiang & Ningjia He

Since a plant miRNA (miR168) cross-regulating a mammalian transcript was reported, miRNA-mediated cross-kingdom communication has become one of the most compelling but controversial topics. In the present study, we used silkworm and mulberry, which is a model for studies on the interactions between the insect and its host plant, to address whether miRNA-mediated cross-kingdom communication is a common phenomenon. The results of TA clone, Sanger sequencing and droplet digital PCR demonstrated that several mulberry-derived miRNAs could enter to silkworm hemolymph and multiple tested tissues. Synthetic miR166b was also detected in hemolymph and fat body. However, the ingestion of synthetic miR166b did not play roles in silkworm physiological progress, which was revealed by RNA-seq analyses, RT-PCR, and phenotypic investigations. Mulberry miRNAs are convincingly transferred to the silkworm orally and no physiological process associated with the miRNAs was demonstrable. The results provided a new aspect of cross-kingdom miRNA transfer.

miRNAs, which are a class of ~22 nt non-coding small RNA molecules, play vital roles by compounding to transcripts of target genes to inhibit translation or degrade mRNA of target genes in animals and plants¹. At present, the studies of miRNAs are mainly focusing on the intracellular miRNAs functions in their own species. For example, miRNAs regulate the growth and development of root, leaf, and flower in plants^{2–4}, and have important roles in the development of organs in animals^{5,6}. Recently, released miRNA was reported to be secreted from cells to body fluid and circulate in body fluid in a surprisingly stable-state in mammals^{7,8}. Those miRNAs could be carried by lipoprotein or other RNA-binding molecules^{9,10}, or packed by microvesicles to deal with the harsh condition (e.g., RNase, and extreme pH)¹⁰. Circulating miRNAs in body fluid were guided to target cells to regulate the expression of target genes^{9,11}.

Recently, miRNA-mediated cross-kingdom communication has become an interesting but controversial topic since it was first reported in 2011¹². Zhang *et al.* discovered that rice-derived miRNAs cross the mammalian gastrointestinal tract to the mouse bloodstream, liver, and other tissues, where they regulate cholesterol levels by reducing the amount of low-density lipoprotein receptor-associated protein 1 (LDLRAP1)¹². These findings provide new insights for genetic regulation by food ingestion and raise the prospect of engineering food or using oral small nucleic acid to prevent or cure diseases^{13,14}. However, in several other recent studies of mice, pigtailed macaques, or insects (*Helicoverpa zea* and *Spodoptera frugiperda*), plant-derived miRNAs were not detected after ingestion of plant-derived food^{13,15,16}. In this context, we used silkworm, *Bombyx mori*, an oligophagous insect that feeds only on mulberry leaves, to study whether mulberry miRNAs can transfer to silkworm upon ingestion. TA clone, Sanger sequencing and droplet digital PCR assay were used to detect mulberry miRNAs in silkworm subset of tissues. RNA-seq was then performed to explore the physiological progresses associated with one of plant miRNA, miR166b, in silkworm.

State Key Laboratory of Silkworm Genome Biology, Southwest University, Beibei, Chongqing 400715, P. R. China. Correspondence and requests for materials should be addressed to N.H. (email: hejia@swu.edu.cn)

miRNA name	Sequence	The reads in the 1 st small RNA library	The reads in the 2 nd small RNA library
mno-miR166c**	UCUCGGACCAGGCUUCAUUC	5	3
mno-miR166b**	UCGGACCAGGCUUCAUUC	2	11
mno-miR167e	UGAAGCUGCCAGCAUGAUCUG	1	1
mno-miR396b	UUCCACAGCUUUCUUGAACUG	1	–
mno-miR159a	UUUGGAUUGAAGGGAGCUCUG	2	–
mno-miR162	UCGAUAAACCUCUGCAUCCAG	1	–
mno-miR156c	UUGACAGAAGAUAGAGACAC	–	2
mno-miR398	UGUGUUCUCAGGUCGCCUG	–	2

Table 1. Eight mulberry miRNAs in silkworm hemolymph identified by solexa sequencing. **miRNAs reported in the mulberry genome by He *et al.*¹⁷. “–” means the relative sequence was not detected in the hemolymph small RNA libraries.

Name	1 st sequencing		2 nd sequencing	
	correct/ Total clones	Rate	correct/ Total clones	Rate
mno-miR169a	2/39	5.13%	0/37	0.00%
mno-miR166b	25/40	62.50%	26/39	66.67%
mno-miR166c	21/37	56.76%	32/46	69.56%
mno-miR167e	27/49	55.10%	15/46	32.61%
mno-miR396b	19/42	45.24%	16/32	50.00%
mno-miR159a	17/24	70.83%	–	–
mno-miR156c	14/39	35.90%	–	–
mno-miR398	20/29	68.97%	–	–
mno-miR162	0/49	0.00%	–	–
mno-miR535	0/38	0.00%	–	–
mno-miR168b	0/42	0.00%	–	–
mno-miR172a	0/39	0.00%	–	–

Table 2. TA-cloning and Sanger sequencing results for mulberry miRNAs identified in silkworm hemolymph. Results are shown for four control mulberry miRNA (mno-miR169a, mno-miR535, mno-miR168b, and mno-miR172a) and the eight mulberry miRNAs (mno-miR166b, mno-miR166c, mno-miR167e and mno-miR396b, mno-miR159a, mno-miR156c, mno-miR398, mno-miR162) in hemolymph. The TA-cloning of the five miRNAs (mno-miR169a, mno-miR166b, mno-miR166c, mno-miR167e, and mno-miR396b) was performed twice. Other miRNAs was performed once. We randomly selected 50 TA-clones for each miRNA for Sanger sequencing, but there were a number of double clones and failed sequencing reactions, so that the total clone number was less than 50. Clones were considered “correct” if the sequence of the clone was identical to the sequence of the corresponding miRNA. The “rate” indicates the sequencing frequency of correct clones relative to the total clones. “–” indicates that we did not clone the miRNA in the hemolymph.

Results

Mulberry-derived miRNAs were detected in silkworm hemolymph. We aligned silkworm hemolymph small RNA sequences (GSE48168)¹⁷ with mulberry miRNAs revealed by next generation sequencing¹⁸. To our surprise, eight mulberry miRNAs (mno-miR166c, mno-miR166b, mno-miR167e, mno-miR396b, mno-miR159a, mno-miR162, mno-miR156c, and mno-miR398) were identified in silkworm hemolymph (Table 1). The reads of these miRNAs were relatively low, with the highest being 11. To ensure that these mulberry-derived miRNAs do not represent contamination during solexa sequencing or sample preparation, we used stem-loop PCR to clone the eight mulberry miRNAs, generating 50 TA-clones for each miRNA, and then subjected them to Sanger sequencing. All of the miRNAs except for mno-miR162 could be detected, with positive clone ratios (perfectly matched clones/total clones) ranging from 35.90% to 70.83% (Table 2, 1st sequencing Hemolymph). Positive clones with incorrect sequences could be explained by the relative low contents of these miRNAs or to homologous silkworm

miRNA name	Fat body (C/T)		Silk gland (C/T)		Brain (C/T)	Prothoracic gland (C/T)	Salivary gland (C/T)	Gut (C/T)	Malpighian tubule (C/T)	Ovary (C/T)	Testis (C/T)
	1st sequencing	2nd sequencing	1st sequencing	2nd sequencing							
mno-miR169a	2.63%	0.00%	0.00%	0.00%	0.00%	2.17%	0.00%	0.00%	0.00%	2.33%	0.00%
mno-miR166b	20.55%	76.19%	56.76%	59.46%	53.66%	31.71%	9.09%	8.57%	10.81%	25.00%	13.33%
mno-miR166c	54.05%	95.45%	72.22%	93.02%	59.52%	61.76%	20.83%	24.39%	42.11%	31.82%	37.50%
mno-miR167e	12.50%	2.27%	13.51%	2.33%	25.64%	9.76%	6.67%	8.11%	20.00%	7.32%	8.16%
mno-miR396b	73.17%	65.96%	55.81%	45.45%	87.23%	66.67%	36.84%	31.71%	48.78%	34.09%	22.44%
mno-miR159a	0.00%	–	5.00%	–	–	–	–	–	–	–	–
mno-miR156c	8.33%	–	2.17%	–	–	–	–	–	–	–	–
mno-miR398	0.00%	–	0.00%	–	–	–	–	–	–	–	–
mno-miR162	0.00%	–	0.00%	–	–	–	–	–	–	–	–

Table 3. TA-cloning and Sanger sequencing results for mulberry miRNAs identified in silkworm tissues. Results are shown for one control mulberry miRNA (mno-miR169a) and four mulberry miRNAs (mno-miR166b, mno-miR166c, mno-miR167e and mno-miR396b) in silkworm tissues (brain, prothoracic gland, salivary gland, gut, malpighian tubule, ovary, testis, fat body, and silk gland). The TA-cloning of the five miRNAs (mno-miR169a, mno-miR166b, mno-miR166c, mno-miR167e, and mno-miR396b) was performed twice in fat body and silk gland, once in other tissues. The percentage represents the sequencing frequency of correct clones relative to the total clones. “–” indicates that we did not clone the miRNA in the fat body, silk gland, brain, prothoracic gland, salivary gland, gut, malpighian tubule, ovary, or testis.

derived small RNAs. As control, we also cloned four mulberry miRNAs that were not identified in the silkworm hemolymph and have varied expression levels in mulberry leaves¹⁸. There were no positive clones for miR535, miR168b, and miR172a (Table 2, 1st sequencing Hemolymph), and the positive clone ratio of miR169a was 5.13%, which is much lower than other seven miRNAs (Table 2, 1st sequencing Hemolymph). These results confirm the specificity of the seven mulberry miRNAs (miR166c, miR166b, miR167e, miR396b, miR159a, miR156c, and miR398). To further confirm these results, we re-cloned miR169a, miR166b, miR166c, miR167e, and miR396b in silkworm hemolymph. The sequencing frequencies of the five miRNAs were similar to those of the first sequencing run (Table 2, 2nd sequencing Hemolymph).

Mulberry-derived miRNAs were detected in multiple silkworm tissues. As the silkworm is a non-vertebrate with an open circulatory system, its organs and tissues are suspended in the hemolymph. To explore whether plant miRNAs enter into the silkworm tissues, the seven mulberry miRNAs were cloned in the fat body and silk gland. The sequencing frequency of four miRNAs (miR166b, miR166c, miR396b, and miR167e) ranged from 12.50% to 73.17% in fat body, and from 13.51% to 72.22% in silk gland, which is significantly higher than frequency of the control, mno-miR169a (2.63% in fat body; 0.00% in silk gland) (Table 3, 1st sequencing Fat body and Silk gland). Repeat sequencing verified the overall trend that mno-miR166b, mno-miR166c and mno-miR396b were more abundant than the control mno-miR169a in the fat body and silk gland, although the frequencies fluctuated in the two experiments (Table 3, 2nd sequencing Fat body and Silk gland). In addition, these four mulberry miRNAs were also cloned in other seven silkworm tissues including brain, prothoracic gland, salivary gland, gut, malpighian tubule, ovary, and testis. The sequencing frequency of four miRNAs (miR166b, miR166c, miR396b, and miR167e) ranged from 25.64%–87.23% in brain, 9.76%–66.67% in prothoracic gland, 6.67%–36.84% in salivary gland, 8.11%–31.71% in gut, 10.81%–48.78% in malpighian tubule, 7.32%–34.09% in ovary, and 8.16%–37.50% in testis, which was more abundant than the control mno-miR169a (Table 3, supplementary Table S1). The results support the assertion that mulberry miRNAs can enter into silkworm tissues.

Synthetic miR166b was detected in silkworm hemolymph and fat body. To further investigate the potential role of miR166b, we synthesized this miRNA with modified 2'-O-methyl on its terminal nucleotide, which is characteristic of plant miRNAs¹⁹, and smeared 300 pmol on a piece of mulberry leaf to feed silkworm larvae. Droplet digital PCR was applied to detect the copy numbers of miR166b in silkworm hemolymph, fat body, and silk gland before and after ingestion. The copy number counts differed over time according to the tissue type (Fig. 1, supplementary Fig. S1 and Table S2). In hemolymph, the miR166b counts peaked at 0.5h and 3h, with 30 and 18 times the count at 0h; the counts at 6h and 12h were similar to those at 0h. The trend in fat body was similar to that in hemolymph. However, the trend in silk gland differed, with miR166b counts at 0.5h, 3h, 6h, and 12h slightly less than the count at 0h. These results suggest that synthetic miR166b could enter to silkworm hemolymph and fat body,

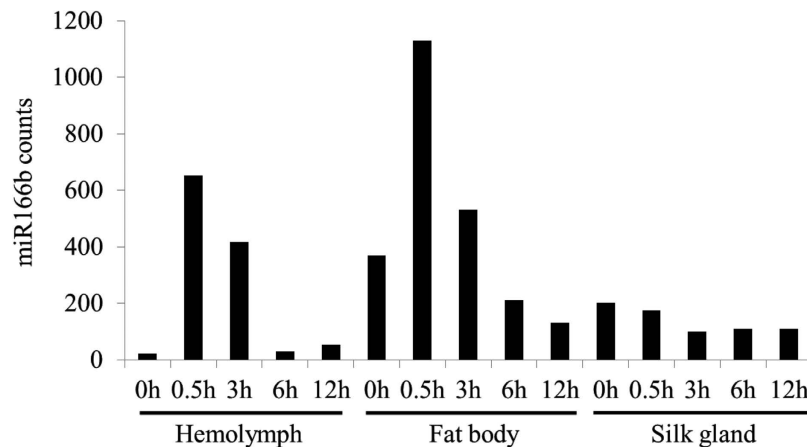


Figure 1. Synthetic miR166b entry into silkworm hemolymph and fat body after silkworm ingestion as determined by droplet digital PCR. The copy number counts of miR166b in 80 ng small RNA of silkworm hemolymph, 240 ng total RNA of fat body, and 240 ng total RNA of silk gland were investigated by droplet digital PCR before (0h) and following ingestion of 300 pmol synthetic miR166b (0.5h, 3h, 6h, and 12h).

but not to silk gland. These results also suggest that it takes 0.5 h or less for synthetic miR166b to enter hemolymph and fat body and that miR166b lasts 3 hours before degradation.

Expression of miR166b potential target genes were not repressed by the synthetic miR166b. To explore the functions of miR166b in silkworm, we predicted the potential target genes for miR166b in silkworm full-length cDNA data using miranda software. With the criteria of energy lower than -25 kcal/mol and perfected “seed region” match, we identified 72 potential target genes of miR166b (data not shown). Eleven best matched target genes, whose energy were lower than -26.84 kcal/mol (supplementary Table S3) were subjected to RT-PCR verification. The results showed the expression levels of these genes were not significantly changed in silkworm fed on synthetic miR166b (Fig. 2, supplementary Fig. S2).

RNA-seq analyses of silkworm fed on synthetic miR166b. For a better understanding of the potential overall biological roles of ingested mno-miR166b in silkworms, we used RNA-seq to reveal the global expression patterns in whole body of silkworm larvae before and after feeding with synthetic miR166b for 3 hours. Compared with silkworm larvae fed on mulberry leaves, only 30 genes were differentially expressed, of which 17 were up-regulated and 13 were down-regulated in larvae feeding with synthetic miR166b. These genes can be classified into seven groups (supplementary Fig. S3, Table 4): immunity (11 genes), response to stress (1 gene), development (5 genes), cytoskeleton (1 gene), digestion (1 gene), hydrolyzing juvenile hormone (1 gene), and unknown function (10 genes). Genes involved in immunity and stress comprised about 40% of the differentially expressed genes. Thus, the ingestion of synthetic miR166b might activate the host response against non-self-molecules. We further fed silkworm larvae with two other synthetic miRNAs, miR166c and miR167e. Six genes randomly chosen from 30 DEGs (Differentially Expressed Genes) were subjected to RT-PCR analyses. The result showed that *Bm_nscaf2556_13* was down-regulated by synthetic miR166c, *Bm_nscaf2818_080* was up-regulated by miR167e, and *Bm_nscaf1071_24* gene was up-regulated by both (Fig. 3). The results indicated that the different expression of these immunity-related genes was caused by the ingestion of nucleic acids, not specific to miR166b. Therefore, we speculate that the ingested synthetic miR166b basically did not play a significant physiological role to *B. mori*. Consistently, there was no significant overlap in the predicted miR166b target sites for the 30 differentially expressed genes (data not shown). In addition, the expression levels of 72 potential target genes for miR166b were not significantly changed in silkworm fed on synthetic miR166b (supplementary table S4). These results suggest that mulberry miR166b has no significant effect on the expression of silkworm genes.

Phenotypic investigation of silkworms fed on synthetic miR166b. We also investigated the phenotypic changes of silkworm feeding on mulberry leaves with and without synthetic miR166b. As shown in Fig. 4, neither the weight (Fig. 4A) nor their wandering rate (Fig. 4B) showed significant difference between two groups. Similar observations had been made in lethality (Fig. 4C). The fat body and silk gland are two major organs in silkworm. The developmental growth of silk gland and fat body can be reflected by the weight of cocoon and pupae, respectively. Since the synthetic miR166b was detected in fat body and not silk gland, we then measured the pupa and cocoon weight at 10 days after ingestion of synthetic miR166b. Results showed that there was no significant difference of pupa and cocoon weight between two groups (Fig. 4D).

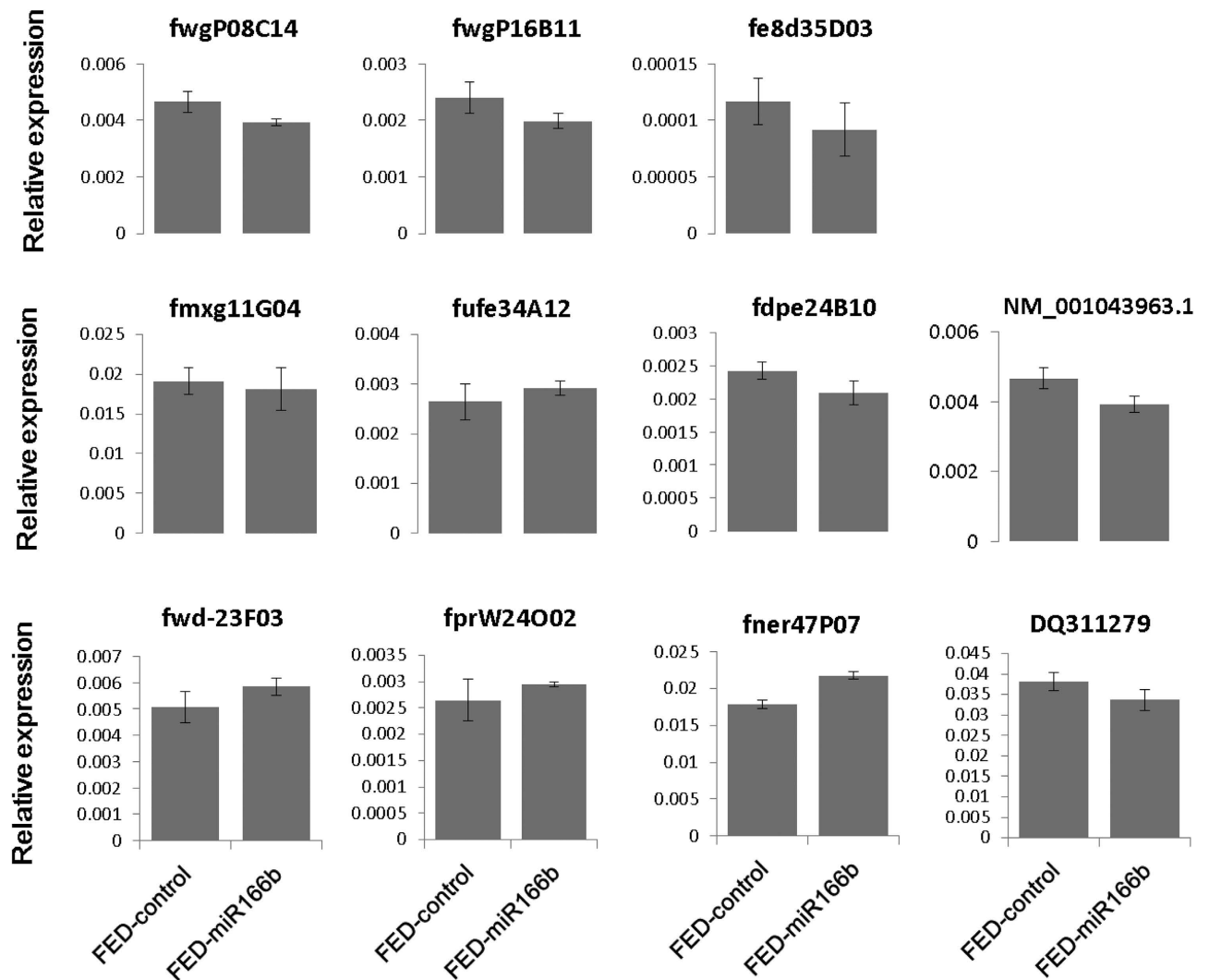


Figure 2. The expression level of 11 potential miR166b target genes in whole body before and after silkworm ingested synthetic miR166b. FED-control represents the silkworm larvae were fed on only mulberry leaves. FED-miR166b means the silkworm larvae were fed on a piece of mulberry leaf containing synthetic miR166b. Statistical significance was determined by Student's t test (* $p < 0.05$).

Discussion

Using T-A clone and Sanger sequencing assay, we revealed that mulberry-derived miRNAs not only transferred to silkworm hemolymph, but also to other tissues such as fat body and silk gland. In addition, droplet digital PCR assay showed that synthetic miR166b also could enter to silkworm hemolymph and fat body after orally feeding. However, RNA-seq analyses, RT-PCR verification, and phenotypic investigation showed that no physiological process in silkworm associated with the ingestion of one tested mulberry miRNA (miR166b). Zhang *et al.* (2012) analyzed small RNA libraries of several species, and they concluded that low reads of plant-derived miRNA detected in animals were from contamination of large-scale sequencing and sample preparation¹⁶. Dickinson *et al.* (2013) applied solexa method to sequence the serum and liver of mice fed with three synthetic food containing different amount of rice¹³. They also emphasized those low reads of plant-derived miRNA in mammal tissues were from contamination¹³. However, the above two studies did not use different methods to detect the plant-derived miRNAs in animals. The methods used in this study are much more rigorous than those of previous studies and the data proved that the mulberry-derived miRNAs detected in silkworm did not result from contamination as following reasons. (1) TA-cloning and Sanger sequencing can rule out the possibility that the mulberry-derived miRNAs in silkworm were from solexa sequencing contamination; (2) Mulberry miRNAs with high expression levels were used as controls and were not detected in the silkworm hemolymph; (3) The identification of synthetic miR166b was confirmed in silkworm tissues after ingestion.

Our results demonstrated that both of mulberry-derived and synthetic plant miRNA were convincingly transferred to silkworm tissues. Zhang *et al.* and Zhou *et al.* recently reported that rice and

Gene ID	FED-control	FED-166b	log ₂ ratio	Up/Down-Regulated	E-value	Annotation (nr database)	Function	Species	References
Bm_scaffold779_2	2.595	0.924	-1.49	Down	0	heat shock protein 68	stress response	<i>H. zea</i>	Zhang and Denlinger, 2010 ²⁴
Bm_nscf2818_080	27.183	57.649	1.085	Up	1.00E-29	protease inhibitor-like protein	immunity	<i>A. mylitta</i>	Gandhe et al. 2006 ²⁵
Bm_nscf3098_40	8.832	52.509	2.572	Up	1.00E-126	gloverin 1 precursor	immunity	<i>B. mori</i>	Kawaoka et al. 2008 ²⁶
Bm_nscf3050_1	0.607	1.886	1.634	Up	0	glucose dehydrogenase [acceptor]-like, partial	immunity	<i>M. sexta</i>	Diana et al. 1994 ²⁷
Bm_nscf2556_12	25.945	65.987	1.347	Up	2.00E-149	attacin precursor	immunity	<i>B. mori</i> <i>H. cecropia</i>	Sugiyama et al. 1995 ²⁸ Carlsson et al. 1991 ²⁹
Bm_nscf1071_24	26.328	61.537	1.225	Up	2.00E-32	cecropin-D precursor	immunity	<i>B. mori</i>	Yang et al. 1999 ³⁰
Bm_nscf2556_13	112.806	232.042	1.041	Up	2e-150	attacin precursor	immunity	<i>B. mori</i>	Sugiyama et al. 1995 ²⁸ Carlsson et al. 1991 ²⁹
Bm_nscf2655_045	2.21	4.466	1.015	Up	1.00E-174	division abnormally delayed protein-like	immunity	<i>Drosophila</i>	Zhu and Zhang, 2013 ³¹
Bm_nscf2970_047	4.009	1.501	-1.417	Down	7.00E-130	mucin-17-like	immunity	<i>Trichoplusia ni</i>	Wang and Granados, 1997 ³²
Bm_nscf2814_10	2.787	1.096	-1.347	Down	0	serine protease inhibitor 19 precursor	immunity	<i>M. sexta</i>	An et al. 2011 ³³
Bm_nscf1071_25	6.426	18.529	1.528	Up	9.00E-31	antibacterial peptide enbocin 2 precursor	immunity	<i>B. mori</i>	Kim et al. 1998 ³⁴ Kaneko et al. 2007 ³⁵
Bm_nscf2883_004	2.746	7.882	1.521	Up	4.00E-58	golgi-specific brefeldin A-resistance guanine nucleotide exchange factor 1-like	immunity	<i>a cell line</i>	Panda D, 2011 ³⁶
Bm_nscf2847_032	7.823	15.792	1.013	Up	1.00E-120	maltase 1-like	digestion	<i>A. gambiae</i> <i>A. aegypti</i>	Zheng et al. 1995 ³⁷ James et al. 1989 ³⁸
Bm_nscf3032_113	0.859	2.096	1.287	Up	0	juvenile hormone esterase-like	hydrolyzing JH, transporting JH	<i>H. virescens</i>	Hanzlik et al. 1989 ³⁹
Bm_nscf2954_01	2.511	0.762	-1.72	Down	0	protein odd-skipped-like	development	<i>Drosophila</i>	Gao et al. 2011 ⁴⁰
Bm_nscf3045_44	1.965	0.59	-1.735	Down	5.00E-73	c-Cbl-associated protein isoform A (CAP)	development	<i>B. mori</i>	Georgomanolis et al. 2009 ⁴¹
Bm_nscf2865_098	1.047	0.309	-1.762	Down	0	LOW QUALITY PROTEIN: voltage-dependent T-type calcium channel subunit alpha-1G-like	development	<i>Drosophila</i>	Dason et al. 2009 ⁴²
Bm_nscf2993_283	2.588	1.053	-1.298	Down	0	synaptotagmin I	development	<i>Drosophila</i>	Yoshihara et al. 2002 ⁴³
Bm_nscf2886_33	0.974	2.736	1.49	Up	0	kinesin-like protein unc-104-like	development	<i>Drosophila</i>	Kern et al. 2013 ⁴⁴
Bm_nscf2883_108	1.58	0.358	-2.14	Down	0	WD repeat-containing protein 67-like	cytoskeleton	<i>Saccharomyces cerevisiae</i>	Walter et al. 2003 ⁴⁵
Bm_nscf2795_061	66.485	21.505	-1.628	Down	0	low molecular mass 30 kDa lipoprotein 19G1-like	unknown	-	-
Bm_nscf2795_060	453.713	146.829	-1.628	Down	0	low molecular mass 30 kDa lipoprotein PBMHP-12-like	unknown	-	-
Bm_nscf2795_062	16.964	5.728	-1.566	Down	0	low molecular mass 30 kDa lipoprotein 21G1-like	unknown	-	-

Continued

Gene ID	FED-control	FED-166b	log ₂ ratio	Up/Down-Regulated	E-value	Annotation (nr database)	Function	Species	References
Bm_nscf2795_064	7.011	2.058	-1.769	Down	0	low molecular mass 30 kDa lipoprotein 19G1-like precursor	unknown	-	-
Bm_nscf3003_019	2.588	9.563	1.885	Up	3.00E-75	actin cytoskeleton-regulatory complex protein PAN1-like	unknown	-	-
Bm_nscf2903_06	2.987	6.29	1.075	Up	2.00E-158	uncharacterized protein LOC101737815	unknown	-	-
Bm_nscf2529_069	1.619	0.663	-1.288	Down	0	uncharacterized protein LOC101738767	unknown	-	-
Bm_scaffold700_2	2.896	6.168	1.091	Up	6.00E-141	neuroligin-2-like	unknown	-	-
Bm_nscf2575_112	0.001	0.714	9.479	Up	1.00E-159	Bardet-Biedl syndrome 1 protein-like	unknown	-	-
Bm_nscf3063_090	3.78	12.138	1.683	Up	5.00E-25	myotubularin-related protein 3-like	unknown	-	-

Table 4. Genes that were differentially expressed before and after silkworms were fed synthetic miR166b. Gene expression levels (reads per kb per million reads, RPKM) were determined prior to feeding (FED-control) or after feeding of synthetic miR166b (FED-miR166b). The “FED-control” and “FED-166b” represents FED-control-RPKM and FED-166b-RPKM, respectively. The “log₂ratio” means log₂ (FED-166b-RPKM/FED-control-RPKM). The “Up/down-regulated” means Up-Down-Regulation (FED_166b/FED_control). *H. zea*, *A. mylitta*, *B. mori*, *M. sexta*, *H. cecropia*, *A. gambiae*, *A. aegypti*, *H. virescens*, and *S. cerevisiae* represent *Helicoverpa zea*, *Antheraea mylitta*, *Bombyx mori*, *Manduca sexta*, *Hyalophora cecropia*, *Anopheles gambiae*, *Aedes aegypti*, *Heliothis virescens*, and *Saccharomyces cerevisiae*, respectively.

honeysuckle-derived miRNAs could be detected in mammalian tissues^{12,20}. Taken their results and our data together, it is undoubtedly believed that plant-derived miRNAs entering to recipient animal organisms is a conserved phenomenon. But nevertheless there are some differences between our observation and Zhang *et al.*' report¹². One is the plant-derived miRNAs detected in silkworm were less than those reported by Zhang *et al.* in mammal¹². A total of seven miRNAs were identified in the silkworm hemolymph and only two plant-derived miRNA (mno-miR166b and mno-miR156c) are common in silkworm and mammals, suggesting that mammals and insects may have different selection encountered the varied plant-derived miRNAs from food. The other is the reads of xenomes from silkworm hemolymph were lower than those from mammals¹². According to the current studies on miRNAs, the functions of miRNAs appear to be associated with their abundances²¹. Gavriel *et al.* reported only the most abundant miRNAs in a cell mediated significant target suppression²¹. Thus, there was a question whether miRNA with low abundance could play roles in physiological processes. Based on our data, the answer is no. Zhang *et al.* found rice miR168 regulated the level of cholesterol by targeting to LDLRAP1¹². Zhou *et al.* reported honeysuckle miR2911 inhibited H1N1-PB2 and AS1 to suppress viral infection²⁰. The abundances of the above two miRNAs (miR168 and miR2911) were very high in mice tissues after ingestion, which may provide the basis for the miRNAs playing roles in mice. Therefore, we can speculate that cross-kingdom miRNA transfer is a conserved phenomenon, however, not all plant-derived miRNAs have influence on the physiological progress of recipient animal organism. It is still unclear how plant-derived miRNAs resist to herbivore RNAses. The differential stability or resistance to RNAses in recipient animal tissues might be crucial for their functions. Further analysis will be required to clarify the underlying mechanism.

Material and Methods

Identification of mulberry-derived miRNAs in silkworm hemolymph. The hemolymph small RNA data of silkworm (GSE48168) was downloaded from NCBI (<http://www.ncbi.nlm.nih.gov/>). Mulberry-derived miRNAs identified from mulberry leaves small RNA library¹⁸ were aligned with silkworm hemolymph small RNA sequences.

Preparations of the silkworm hemolymph and tissue samples. Silkworm larvae were fed mulberry leaves under a 12h-light/12h-dark cycle at 25 °C with relative humidity of 75%. Silkworm hemolymph was collected from fifth instar day-5 larvae using sterile tubes containing a few crystals of phenylthiourea. The silkworm larvae were dissected. The brain, prothoracic gland, salivary gland, gut, malpighian tubule, ovary, testis, fat body, and silk gland samples were collected and washed three times

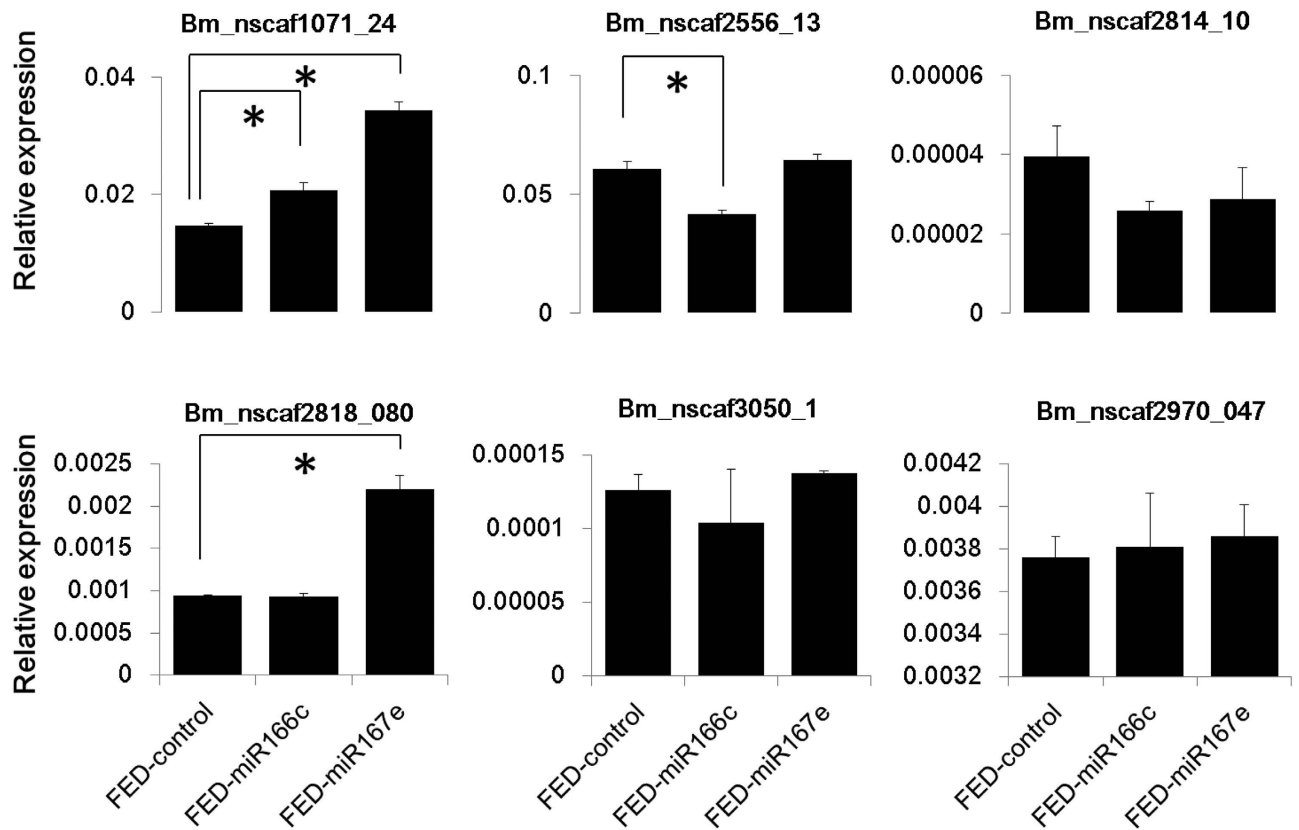


Figure 3. The expression level of 6 differentially expressed genes in silkworm ingested synthetic miR166c and miR167e. Differentially expressed genes were identified by transcriptome analysis. FED-control represents the silkworm larvae were fed on only mulberry leaves. FED-miR166c and FED-miR167e means the silkworm larvae were fed on a piece of mulberry leaf containing synthetic miR166c and miR167e, respectively. Statistical significance was determined by Student's t test (* $p < 0.05$).

with cold 0.75% NaCl. Hemolymph samples were centrifuged at $3000 \times g$ for 10 min at 4°C . The supernatants of hemolymph, tissue samples were stored at -80°C until use.

Tissues from silkworms fed synthetic miR166b. 300 pmol of synthetic miR166b (UCGGACCAGGCUUCAUCCCC) with a 2'-O-methyl modified terminal nucleotide (RIBOBIO, China) was daubed on $\sim 1\text{ cm}^2$ pieces of mulberry leaf. The synthetic miR166b was dissolved in RNase-free water. A single piece of leaf was fed to each silkworm larvae in the fifth instar day-5 after the miRNA liquid dried. The hemolymph, fat body, and silk gland were collected at 0.5 h, 3 h, 6 h and 12 h after the larvae ate the whole piece of leaf. Control (0 h) silkworms were only fed mulberry leaves. Each group contained five larvae.

RNA extraction, T-A cloning and Sanger sequencing. Total RNA from the fat body and silk gland was extracted using RNAiso Plus (D9108A, Takara, China) according to the manufacturer's instructions. The small RNA was purified using mirVana™ PARIS™ Kit (AM1556, Ambion, USA) and eluted in $25\ \mu\text{l}$ non-nuclease water. Total RNA from fat body and silk gland and small RNA from hemolymph were reverse transcribed to cDNA in $10\ \mu\text{l}$ reactions using M-MLV (D2641B, Takara, China) and specific reverse transcriptional primers for each miRNA. Stem-loop PCR was performed using miRNA specific forward and reverse primers (supplementary Table S5). The PCR products were cloned into pMD19-T vector (D102A, Takara, China). We randomly picked 60 monoclones for each miRNA, and of these, chose 50 clones that could be verified by bacterial PCR for Sanger sequencing with M13 primer.

Measurement of miRNA copy number counts by droplet digital PCR. To standardize the amount of tissue at five time points, we reverse transcribed the same amount of total RNA from the silk gland and fat body, or small RNA from hemolymph at each time point. Total RNA ($2.4\ \mu\text{g}$) from silkworm fat bodies or silk glands, or small RNA (800 ng) from hemolymph before or after oral synthetic miR166b at each of five time points was reverse transcribed in $15\ \mu\text{l}$ reactions using the TaqMan

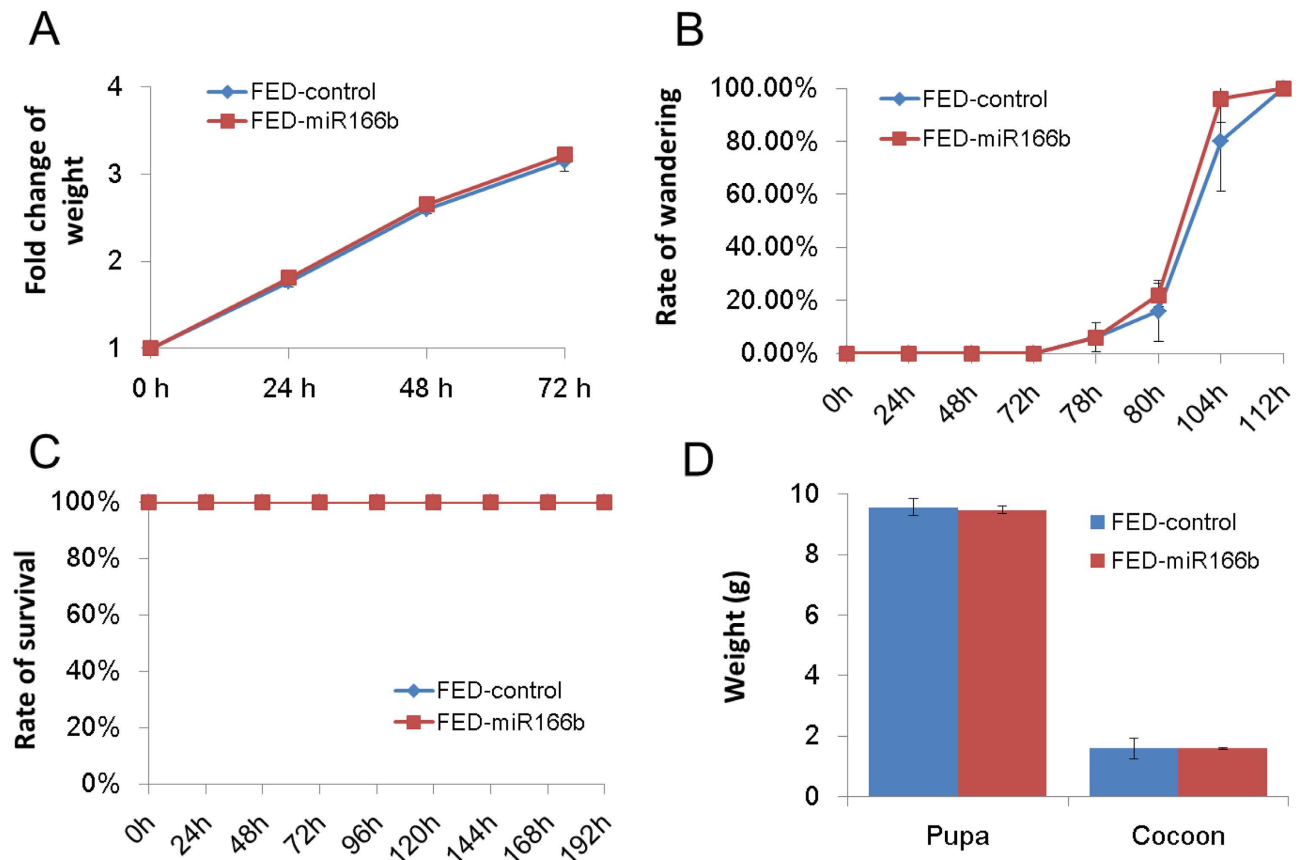


Figure 4. The phenotypic investigation of silkworm larvae fed on mulberry leaves with/without synthetic miR166b. The phenotypic investigation including larva weight (A), rate of wandering (B), rate of survival (C), pupa and cocoon weight (D) were measured before (0 h) and after silkworm ingested synthetic miR166b (24 h, 48 h, 72 h, 96 h, 120 h, 144 h, 168 h, and 192 h). Fold change of weight means the ratio of larvae weight after silkworm ingested synthetic miR166b (24 h, 48 h, 72 h) divided the larvae weight at 0 h. Rate of wandering indicates the percentage of silkworm developed into the wandering stage. FED-control represents the silkworm larvae were fed only on mulberry leaves. FED-miR166b means the silkworm larvae were fed on a piece of mulberry leaf containing synthetic miR166b. Statistical significance was determined by Student's t test ($*p < 0.05$).

microRNA reverse transcription kit (43366596, ABI, USA). ddPCR was performed using the QX100 droplet generator and droplet reader. Each PCR reaction was carried out in a 20 μ l volume containing 10 μ l 2X ddPCR supermix (Bio-rad, USA), 1.5 μ l cDNA, 1 μ l miR166b-specific hydrolysis probe assay (4427975, Life Technologies, USA), and 7.5 μ l non-nuclease water. The 20 μ l reaction was divided by the droplet generator and detected by the droplet readers according to the manufacturer's instructions.

Materials for RNA-seq. The 450 pmol synthetic miR166b (UCGGACCAGGCUUCAUCCCC) with 2'-O-methyl modification on its terminal nucleotide (RIBOBIO, China) was daubed on a ~ 1 cm² piece of mulberry leaf. Piece of leaf were fed to silkworm larvae in the fifth instar day-2 after the miRNA liquid dried. Whole silkworm larvae were collected at 3 h after ingestion of an entire piece leaf, and this experimental group (FED-miR166b) was stored at -80°C until use. A control group of silkworm (FED-control) was only fed mulberry leaves. Each group contained three larvae. Total RNA from whole larvae were extracted by RNAiso Plus (D9108A, Takara, China) according to manufacturer's instructions. Agilent 2100 was used to ensure the integrity of total RNA. cDNA libraries were constructed using the TruSeq RNA Sample Preparation v2 Guide (Illumina), and then sequenced by Illumina HiSeqTM 2000. The obtained raw data from solexa sequencing were deposited on the Short Read Archive of NCBI (<http://www.ncbi.nlm.nih.gov/sra/>) with accession number SRP051555.

Transcriptome analysis before and after silkworm larvae were fed synthetic miR166b. The quality of raw data in the FED-control and FED-miR166b transcriptome was determined by CLC Genomics Workbench 5.5 following the manufacturer's instructions. After filtering the low quality, the clean reads were obtained that matched the silkworm genome and silkworm genes (<http://www.silkdb>).

org/silkdb/doc/download.html) by SOAP2^{22,23}. The distribution and coverage of clean reads on the silkworm genome and genes were analyzed using CLC Genomics Workbench 5.5. Expression analysis of each gene in two transcriptomes was performed as follows. Briefly, the expression level of each gene was normalized using the reads per kb per million reads (RPKM) method²⁴. P value < 0.05 and false discovery rate (FDR) < 0.001 were used as thresholds for gene expression. Genes with absolute values of the log₂ of the ratio of RPKMs (FED-miR166b/FED-control) that were more than 1 were regarded as a differentially expressed. Values of more than 1 indicated up-regulated genes, and values of less than -1 indicated down-regulated genes. The annotations of differentially expressed genes were performed by aligning against the non-redundant protein sequences (nr) database using BLASP (http://blast.st.va.ncbi.nlm.nih.gov/Blast.cgi?PROGRAM=blastp&PAGE_TYPE=BlastSearch&LINK_LOC=blasthome).

Target site prediction for 30 differentially expressed genes and silkworm full-length cDNA for miR166b. Silkworm full-length cDNA sequences were downloaded from KAIKObase (<http://sgp.dna.affrc.go.jp/FLcDNA/>). Target sites prediction for 30 differentially expressed genes and silkworm full-length cDNA for miR166b was performed using Miranda software (<http://www.microrna.org/microrna/getDownloads.do>). The criteria were set as follows. (1) The “seed region” of miR166b (containing the 2nd to 8th nucleotides of the mature miRNA from 5' to 3') should match the target genes (30 differentially expressed genes) with perfect complementary. (2) The free energy of the hybrid should be less than -25 kcal/mol.

RT-PCR detection of potential target genes. The 450 pmol synthetic miR166c (UCUCGGACCAGGCUUCAUCC) and synthetic miR167e (UGAAGCUGCCAGCAUGAUCUG) with 2'-O-methyl modification on their terminal nucleotides (RIBOBIO, China) were fed to silkworm larvae as above described. Each group contained three larvae. The larvae in control group (FED-control) were only fed on mulberry leaves. Total RNA of FED-miR166b, FED-miR166c, FED-miR167e, and FED-control from whole larvae were extracted by RNAiso Plus (D9108A, Takara, China) according to manufacturer's instructions. Total RNA were reverse transcribed to cDNA by using PrimeScript RT reagent Kit with gDNA Eraser (RR047A, Takara, China). The cDNA was then diluted four times and used as the template to perform the RT-PCR with gene specific forward and reverse primers, as listed in supplementary Table S6. The PCR reactions were performed in ABI Step One Plus (Applied Biosystems, USA) using SYBR Premix Ex TaqTM II (RR820A, Takara, China) as the following conditions: 95 °C for 30 s, 40 cycles of 95 °C for 5 s, and 60 °C for 30 s. The translation initiation factor 4A was used as an inner control. All reactions were assayed in triplicated. The relative expression level of genes was calculated using 2^{-ΔΔCt} method.

Phenotypic investigation of silkworm larvae fed on mulberry leaves with/without synthetic miR166b. The FED-miR166 and FED-control groups contained five sub-groups, separately, and each sub-group contained 10 larvae. The weight of larva, rate of wandering, and rate of survival in each groups were investigated. The weight of pupa and cocoon were measured at 10 days after ingestion of synthetic miR166b. Student's t test (*p < 0.05) was performed to determine the statistical significance according to the graphpad software (<http://www.graphpad.com/quickcalcs/ttest1.cfm>).

References

- Bartel, D. P. MicroRNAs: genomics, biogenesis, mechanism, and function. *cell* **116**, 281–297 (2004).
- Khan, G. A. *et al.* MicroRNAs as regulators of root development and architecture. *Plant Mol Biol* **77**, 47–58 (2011).
- Kidner, C. A. The many roles of small RNAs in leaf development. *J Genet Genomics* **37**, 13–21 (2010).
- Luo, Y., Guo, Z. & Li, L. Evolutionary conservation of microRNA regulatory programs in plant flower development. *Dev Biol* **380**, 133–144 (2013).
- Ryazansky, S., Mikhaleva, E. & Olenkina, O. Essential functions of microRNAs in animal reproductive organs. *Mol Biol* **48**, 319–331 (2014).
- Waldron, J. & Newbury, S. The roles of miRNAs in wing imaginal disc development in *Drosophila*. *Biochem Soc T* **40**, 891 (2012).
- Chim, S. S. *et al.* Detection and characterization of placental microRNAs in maternal plasma. *Clin Chem* **54**, 482–490 (2008).
- Mitchell, P. S. *et al.* Circulating microRNAs as stable blood-based markers for cancer detection. *P Natl Acad Sci USA* **105**, 10513–10518 (2008).
- Vickers, K. C., Palmisano, B. T., Shoucri, B. M., Shamburek, R. D. & Remaley, A. T. MicroRNAs are transported in plasma and delivered to recipient cells by high-density lipoproteins. *Nat Cell Biol* **13**, 423–433 (2011).
- Javidi, M. A. *et al.* Cell-free microRNAs as cancer biomarkers: the odyssey of miRNAs through body fluids. *Med Oncol* **31**, 1–11 (2014).
- Zhang, Y. *et al.* Secreted monocytic miR-150 enhances targeted endothelial cell migration. *Mol Cell* **39**, 133–144 (2010).
- Zhang, L. *et al.* Exogenous plant MIR168a specifically targets mammalian LDLRAP1: evidence of cross-kingdom regulation by microRNA. *Cell Res* **22**, 107–126 (2011).
- Dickinson, B. *et al.* Lack of detectable oral bioavailability of plant microRNAs after feeding in mice. *Nat Biotechnol* **31**, 965–967 (2013).
- Hirschi, K. D. New foods for thought. *Trends Plant Sci* **17**, 123–125 (2012).
- Witwer, K. W., McAlexander, M. A., Queen, S. E. & Adams, R. J. Real-time quantitative PCR and droplet digital PCR for plant miRNAs in mammalian blood provide little evidence for general uptake of dietary miRNAs: limited evidence for general uptake of dietary plant xenomiRs. *RNA Biol* **10**, 1080–1086 (2013).
- Zhang, Y. *et al.* Analysis of plant-derived miRNAs in animal small RNA datasets. *BMC Genomics* **13**, 381 (2012).
- He, N. *et al.* Draft genome sequence of the mulberry tree *Morus notabilis*. *Nat Commun* **4** (2013).

18. Jia, L. *et al.* Identification of the Conserved and Novel miRNAs in Mulberry by High-Throughput Sequencing. *PLoS One* **9**, e104409 (2014).
19. Chen, X. Small RNAs and their roles in plant development. *Annu Rev Cell Dev Bi* **25**, 21–44 (2009).
20. Zhou, Z. *et al.* Honeysuckle-encoded atypical microRNA2911 directly targets influenza A viruses. *Cell Res* **25**, 39–49 (2014).
21. Mullokkandov, G. *et al.* High-throughput assessment of microRNA activity and function using microRNA sensor and decoy libraries. *Nat Methods* **9**, 840–846 (2012).
22. Li, R. *et al.* SOAP2: an improved ultrafast tool for short read alignment. *Bioinformatics* **25**, 1966–1967 (2009).
23. Mortazavi, A., Williams, B. A., McCue, K., Schaeffer, L. & Wold, B. Mapping and quantifying mammalian transcriptomes by RNA-Seq. *Nat Methods* **5**, 621–628 (2008).
24. Zhang, Q. & Denlinger, D. L. Molecular characterization of heat shock protein 90, 70 and 70 cognate cDNAs and their expression patterns during thermal stress and pupal diapause in the corn earworm. *J Insect Physiol* **56**, 138–150 (2010).
25. Gandhe, A. S., Arunkumar, K., John, S. H. & Nagaraju, J. Analysis of bacteria-challenged wild silkworm, *Antheraea mylitta* (Lepidoptera) transcriptome reveals potential immune genes. *BMC Genomics* **7**, 184 (2006).
26. Kawaoka, S. *et al.* Functional analysis of four Gloverin - like genes in the silkworm, *Bombyx mori*. *Arch Insect Biochem* **67**, 87–96 (2008).
27. Cox-Foster, D. L. & Stehr, J. E. Induction and localization of FAD-glucose dehydrogenase (GLD) during encapsulation of abiotic implants in *Manduca sexta* larvae. *J Insect Physiol* **40**, 235–249 (1994).
28. Sugiyama, M. *et al.* Characterization of a *Bombyx mori* cDNA encoding a novel member of the attacin family of insect antibacterial proteins. *Insect Biochem Molec* **25**, 385–392 (1995).
29. Carlsson, A., Engström, P., Palva, E. T. & Bennich, H. Attacin, an antibacterial protein from *Hyalophora cecropia*, inhibits synthesis of outer membrane proteins in *Escherichia coli* by interfering with *omp* gene transcription. *Infect Immun* **59**, 3040–3045 (1991).
30. Yang, J. *et al.* cDNA cloning and gene expression of cecropin D, an antibacterial protein in the silkworm, *Bombyx mori*. *Comp Biochem Phys B* **122**, 409–414 (1999).
31. Zhu, F. & Zhang, X. The Wnt signaling pathway is involved in the regulation of phagocytosis of virus in *Drosophila*. *Sci Rep* **3** (2013).
32. Wang, P. & Granados, R. R. An intestinal mucin is the target substrate for a baculovirus enhancer. *P Natl Acad Sci USA* **94**, 6977–6982 (1997).
33. An, C., Ragan, E. J. & Kanost, M. R. Serpin-1 splicing isoform J inhibits the proSpätzle-activating proteinase HP8 to regulate expression of antimicrobial hemolymph proteins in *Manduca sexta*. *Dev Comp Immunol* **35**, 135–141 (2011).
34. Kim, S. H. *et al.* Cloning and Expression of a Novel Gene Encoding a New Antibacterial Peptide from Silkworm, *Bombyx mori*. *Biochem Biophys Res Commun* **246**, 388–392 (1998).
35. Kaneko, Y., Furukawa, S., Tanaka, H. & Yamakawa, M. Expression of antimicrobial peptide genes encoding Enbocin and Gloverin isoforms in the silkworm, *Bombyx mori*. *Biosci Biotech Biochem* **71**, 2233–2241 (2007).
36. Panda, D. *et al.* RNAi screening reveals requirement for host cell secretory pathway in infection by diverse families of negative-strand RNA viruses. *P Natl Acad Sci USA* **108**, 19036–19041 (2011).
37. Zheng, L., Whang, L. H., Kumar, V. & Kafatos, F. C. Two genes encoding midgut-specific maltase-like polypeptides from *Anopheles gambiae*. *Exp Parasitol* **81**, 272–283 (1995).
38. James, A. A., Blackmer, K. & Racioppi, J. V. A salivary gland-specific, maltase-like gene of the vector mosquito, *Aedes aegypti*. *Gene* **75**, 73–83 (1989).
39. Hanzlik, T. N., Abdel-Aal, Y., Harshman, L. G. & Hammock, B. D. Isolation and sequencing of cDNA clones coding for juvenile hormone esterase from *Heliothis virescens*. Evidence for a catalytic mechanism for the serine carboxylesterases different from that of the serine proteases. *J Biol Chem* **264**, 12419–12425 (1989).
40. Gao, H., Wu, X. & Fossett, N. Odd-skipped maintains prohemocyte potency and blocks blood cell development in *Drosophila*. *Genesis* **49**, 105–116 (2011).
41. Georgomanolis, T., Iatrou, K. & Swevers, L. BmCAP, a silkworm gene encoding multiple protein isoforms characterized by SoHo and SH3 domains: Expression analysis during ovarian follicular development. *Insect Biochem Molec* **39**, 892–902 (2009).
42. Dason, J. S. *et al.* Frequenin/NCS-1 and the Ca²⁺-channel α 1-subunit co-regulate synaptic transmission and nerve-terminal growth. *J Cell Sci* **122**, 4109–4121 (2009).
43. Yoshihara, M. & Littleton, J. T. Synaptotagmin I functions as a calcium sensor to synchronize neurotransmitter release. *Neuron* **36**, 897–908 (2002).
44. Kern, J. V., Zhang, Y. V., Kramer, S., Brenman, J. E. & Rasse, T. M. The Kinesin-3, Unc-104 regulates dendrite morphogenesis and synaptic development in *Drosophila*. *Genetics* **195**, 59–72 (2013).
45. Voegtli, W. C., Madrona, A. Y. & Wilson, D. K. The structure of Aip1p, a WD repeat protein that regulates Cofilin-mediated actin depolymerization. *J Biol Chem* **278**, 34373–34379 (2003).

Acknowledgements

This project was funded by the research grants from the National Hi-Tech Research and Development Program of China (No. 2013AA100605-3), the Fundamental Research Funds for the Central Universities (No. 2362014xk05), the “111” Project (B12006), and the Science Fund for Distinguished Young Scholars of Chongqing (Grant No. cstc2011jjq0010).

Author Contributions

J.L. and H.N.J. conceived and designed the study. J.L. and Z.D.Y. performed all the experiments. J.L., X.Z.H. and H.N.J. analyzed all the experiments. J.L. and H.N.J. wrote the manuscript with support from all authors.

Additional Information

Supplementary information accompanies this paper at <http://www.nature.com/srep>

Competing financial interests: The authors declare no competing financial interests.

How to cite this article: Jia, L. *et al.* Nonfunctional ingestion of plant miRNAs in silkworm revealed by digital droplet PCR and transcriptome analysis. *Sci. Rep.* **5**, 12290; doi: 10.1038/srep12290 (2015).



This work is licensed under a Creative Commons Attribution 4.0 International License. The images or other third party material in this article are included in the article's Creative Commons license, unless indicated otherwise in the credit line; if the material is not included under the Creative Commons license, users will need to obtain permission from the license holder to reproduce the material. To view a copy of this license, visit <http://creativecommons.org/licenses/by/4.0/>